haematologica
Journal of the Ferrata Storti Foundation

Secondary T-cell lymphoma arising from pre-existing clones in a patient with diffuse large B-cell lymphoma during epcoritamab treatment following CAR-T therapy

by Takuya Terakawa, Shigeo Fuji, Henyun Shi, Yuka Amemiya, Wataru Nakahara, Yoshiki Matsuoka, Yuma Tada, Yasuhiro Shingai, Sayako Yuda, Jun Ishikawa, Hidetoshi Satomi, Hiraku Murakami, Makiko Suga, Naoki Hosen, Yasuhito Nannya, Seishi Ogawa and Takafumi Yokota

Received: September 26, 2025.
Accepted: December 18, 2025.

Citation: Takuya Terakawa, Shigeo Fuji, Henyun Shi, Yuka Amemiya, Wataru Nakahara, Yoshiki Matsuoka, Yuma Tada, Yasuhiro Shingai, Sayako Yuda, Jun Ishikawa, Hidetoshi Satomi, Hiraku Murakami, Makiko Suga, Naoki Hosen, Yasuhito Nannya, Seishi Ogawa and Takafumi Yokota. Secondary T-cell lymphoma arising from pre-existing clones in a patient with diffuse large B-cell lymphoma during epcoritamab treatment following CAR-T therapy.
Haematologica. 2025 Dec 24. doi: 10.3324/haematol.2025.289269 [Epub ahead of print]

Article Category

Case Report

Title

Secondary T-cell lymphoma arising from pre-existing clones in a patient with diffuse large B-cell lymphoma during epcoritamab treatment following CAR-T therapy

Running head: Secondary T-cell lymphoma after CAR-T therapy

Authors

Takuya Terakawa[1,2], Shigeo Fuji[1], Henyun Shi[1], Yuka Amemiya[1], Wataru Nakahara[1], Yoshiki Matsuoka[1], Yuma Tada[1], Yasuhiro Shingai[1], Sayako Yuda[1], Jun Ishikawa[1], Hidetoshi Satomi[3], Hiraku Murakami[2], Makiko Suga[2], Naoki Hosen[2], Yasuhito Nannya[4,5], Seishi Ogawa[4,6,7], and Takafumi Yokota[1,8]

[1]Department of Hematology, Osaka International Cancer Institute, Osaka, Japan

[2]Department of Hematology and Oncology, The University of Osaka, Suita, Japan

[3]Department of Diagnostic Pathology and Cytology, Osaka International Cancer Institute, Osaka, Japan

[4]Department of Pathology and Tumor Biology, Kyoto University, Kyoto, Japan

[5]Division of Hematopoietic Disease Control, The Institute of Medical Science, The University of Tokyo, Tokyo, Japan

[6]Institute for the Advanced Study of Human Biology (WPI-ASHBi), Kyoto University, Kyoto, Japan

[7]Department of Innovative Medicine, Faculty of Medicine, Kindai University, Osakasayama, Japan

[8]Department of Oncology, Graduate School of Medicine, The University of Osaka, Suita, Japan

Authorship Contributions

TT, SF, and TY conceptualized the study and drafted the manuscript. TT, SF, YA, WN, YM, YT, YS, SY, JI, and TY were involved in patient care and clinical management. HSh performed and analyzed the PCR for *TRG* gene and analyzed the Sanger sequencing data of *TRG* and *TP53*. HSa contributed to pathological evaluation and diagnostic interpretation. HM, MS, and NH performed and analyzed the FCM and the qRT-PCR for CD19-CAR. YN and SO contributed to the analysis and interpretation of the NGS data. All authors reviewed and approved the final version of the manuscript.

Corresponding author: Shigeo Fuji, MD, PhD.

Mailing address: Department of Hematology, Osaka International Cancer Institute, 3-1-69, Otemae, Chuo-ku, Osaka city, Osaka, 5418567, Japan

Email: fujishige1231@gmail.com

Phone: +81(6)6945-1181

Fax: +81(06)6945-1900

Data Sharing Statement

The datasets generated during and/or analyzed during the current study are available from the corresponding author upon reasonable request.

Acknowledgments

We would like to thank Enago for professional English language editing of the manuscript.

Funding

None.

Disclosure

Naoki Hosen has received honoraria from Chugai Pharmaceutical Co., Ltd., Janssen Pharmaceutical, Bristol Myers Squibb Co., Takeda Pharmaceutical Co., Ltd., and Novartis Pharma K.K.; research funding from Otsuka Pharmaceutical Co., Ltd., Chugai Pharmaceutical Co., Ltd., Shionogi & Co., Ltd., and Miyarisan Pharmaceutical Co., Ltd.; and grant funding from Chugai Pharmaceutical Co., Ltd., Kyowa Kirin Co., Ltd., Shionogi & Co., Ltd., Asahi Kasei Pharma Corporation, Otsuka Pharmaceutical Co., Ltd., and Takeda Pharmaceutical Co., Ltd. Seishi Ogawa holds leadership and advisory roles with Eisai Co., Ltd., Chordia Therapeutics Inc., and Montage Bio, Inc., and is a shareholder in Asahi Genomics Co., Ltd. S.O. has also received honoraria from The Mitsubishi Foundation and the Nakatani Foundation, and grant/research funding from Chordia Therapeutics Inc., Eisai Co., Ltd., Nanpu Hospital, and Nippon Shinyaku Co., Ltd. Yasuhito Nannya has received honoraria from Bristol Myers Squibb Co., Ltd. and Otsuka Pharmaceutical Co., Ltd. The remaining authors declare no competing financial interests related to this study.

Main Text

In recent years, immune effector cell (IEC) therapies, including chimeric antigen receptor T-cell (CAR-T) therapy and T-cell engaging bispecific antibodies (BsAbs), have emerged as effective treatments for relapsed or refractory hematologic malignancies. Among these, BsAbs targeting CD3 and CD20, such as epcoritamab, have demonstrated efficacy in patients with relapsed or refractory large B-cell lymphoma, including those who have failed prior CAR-T therapy.[1] Although cytokine release syndrome (CRS) is a well-characterized complication of IEC therapies, hemophagocytic lymphohistiocytosis (HLH), also referred to as IEC-associated HLH-like syndrome (IEC-HS), has increasingly been observed.[2] Furthermore, secondary T-cell lymphomas have been reported after CAR-T therapy.[3-8]

We report a rare case of concurrent HLH and secondary T-cell lymphoma in a patient previously treated with CAR-T therapy followed by epcoritamab. Clinical specimens were analyzed, including residual material from the lymphocyte apheresis procedure, as well as peripheral blood and bone marrow samples with secondary T-cell lymphoma involvement (**Figure 1**). This study was conducted in accordance with the Declaration of Helsinki, and written informed consent was obtained from the patient.

A Japanese man in his 40s was diagnosed with diffuse large B-cell lymphoma (DLBCL) in 2009 and achieved complete remission after R-CHOP, followed by autologous stem cell transplantation in 2010 after first relapse treated with R-ICE. He remained in remission until 2022, when nodal relapse occurred and was treated with R-GCD, radiation, and CAR-T therapy with tisagenlecleucel, achieving complete remission. In December 2023, gastrointestinal relapse was confirmed, showing limited response to sobuzoxane and rituximab (**Figure 1**).

Consequently, epcoritamab, a CD3 × CD20 BsAb, was initiated in February 2024, with escalating doses of 0.16 mg on day 1, 0.8 mg on day 8, and 48 mg on day 16. CRS developed following administration of the full dose and was managed with tocilizumab. After the CRS subsided, a second 48 mg dose was administered on day 26. However, a high fever recurred, necessitating additional tocilizumab, but the patient developed persistent fever, pancytopenia, elevated lactate dehydrogenase (LDH), liver dysfunction, hypofibrinogenemia (87 mg/dL), and hyperferritinemia (3,874 μg/L, peaking at 21,376 μg/L). Peripheral blood smears revealed abnormal lymphocytes. On day 41 of epcoritamab therapy, bone marrow analysis identified an abnormal lymphoid infiltration with hemophagocytosis (**Figure 2A**). The patient fulfilled seven of the eight HLH-2004 diagnostic criteria,[9] including fever, splenomegaly, cytopenia, hyperferritinemia, elevated soluble CD25 levels (10,400 U/mL), hypofibrinogenemia, and hemophagocytosis in the bone marrow. In the absence of definitive evidence for autoimmune disease or bacterial, fungal, or other viral infections, including Epstein–Barr virus (EBV) with undetectable DNA in the peripheral blood, and aside from cytomegaloviremia, IEC-HS was suspected, and dexamethasone was initiated on day 41, along with transfusions of red blood cells, platelets, and fresh frozen plasma, resulting in transient clinical improvement. Although liver function, LDH levels, and high fever temporarily improved with treatment, and dexamethasone was tapered, these symptoms recurred on day 71, raising concern for HLH relapse. Despite the addition of etoposide and high-dose corticosteroids, the patient's condition deteriorated, and he ultimately died of multiorgan failure on day 80 (**Figure 1**).

Bone marrow flow cytometry (FCM) on day 41 revealed an aberrant T-cell population characterized by CD8 positivity, CD5 negativity, and dim CD7 expression (**Figure 2B**).

Histopathological examination of the bone marrow clot section revealed infiltration of CD3-positive lymphoid cells with irregular nuclear contours. CD8-positive cells showed a distribution corresponding to CD3-positive cells (**Figure 2C**), and BCL6 expression was observed in the same population. TIA-1- and granzyme B-positive lymphocytes increased, accompanied by clusters of CD68- and CD163-positive macrophages. CD10- and PD-1-positive cells were observed but did not colocalize with CD3-positive cells. CD30- or CD56-positive cells were absent, and *in situ* hybridization for EBV-encoded RNA was negative. Additionally, *T-cell receptor* (*TCR*) gene rearrangement was detected by polymerase chain reaction (PCR), indicating clonal T-cell proliferation.

We assessed CAR expression in the abnormal T-cells by FCM and quantitative reverse transcription PCR (qRT-PCR) at the University of Osaka. FCM of peripheral blood collected on day 43 of epcoritamab therapy, approximately 30% of the mononuclear cells were CD8-positive and CD5-negative, consistent with the same immunophenotype as the abnormal T-cells in the bone marrow, showed no detectable surface expression of CAR (**Figure 3A**). Concurrent qRT-PCR using the same specimen also failed to detect CAR transgene transcripts. These results indicate that the abnormal T-cells were not derived from the CAR-T product.

To further characterize the abnormal T-cells, targeted next-generation sequencing (NGS) was performed on a bone marrow sample collected on day 76. Targeted NGS was conducted at Kyoto University using an in-house panel covering 434 genes recurrently mutated in lymphoid malignancies, with a sensitivity of approximately 2% variant allele frequency. This revealed two structural deletions associated with the *TCR gamma* (*TRG*) gene rearrangement and a *TP53* nonsense mutation p.R213X (c.637C>T), accompanied by copy number variation (**Figure 3B**).

To determine whether the abnormal T-cell clone existed prior to CAR-T manufacturing, we analyzed the peripheral blood apheresis sample. Using primers targeting the *TRG* deletion site identified by NGS, qualitative PCR detected the identical clones in both the apheresis sample and the bone marrow sample with T-cell lymphoma involvement (**Figure 3C**). The PCR products were excised from the gel and subjected to Sanger sequencing, which confirmed identical junction sequences (**Figure 3D**), indicating that the abnormal T-cell clone was already present before CAR-T manufacturing. We also sorted and examined CD3-positive and CD3-negative cells from the apheresis sample, and PCR revealed the identical *TRG* amplicon in CD3-positive cells, but not in CD3-negative cells (**Figure 3C**), excluding the possibility that the *TRG* deletion resulted from a germline polymorphism. Sanger sequencing of the *TP53* c.637C>T locus demonstrated that the mutation was absent in the apheresis sample, suggesting it was acquired during CAR-T or epcoritamab therapy (**Figure 3E**).

Based on the histopathology, the rearrangement of clonal *TCR*, and the *TP53* mutation, the diagnosis of peripheral T-cell lymphoma, not otherwise specified, was made according to the World Health Organization classification of haematolymphoid tumours (5th edition),[10] as no specific features of other mature T-cell lymphoma subtypes were identified. While clonal T-cell proliferation is frequently observed in HLH, especially EBV-associated cases,[11] we found no evidence of EBV involvement in this patient.

This case is notable for the development of secondary T-cell lymphoma with concurrent HLH during epcoritamab therapy following prior CAR-T treatment. The clinical course suggests that IEC therapies may have contributed to the expansion of a latent T-cell clone. Given that similar cases have been reported,[3,6,12] clinicians should remain vigilant for underlying T-cell malignancies when evaluating patients with suspected IEC-HS.

Concerns have been raised that CAR-T therapy may increase the risk of secondary T-cell lymphomas due to the use of lentiviral vectors or genetic engineering. However, the current evidence does not support a significantly elevated risk specifically attributable to CAR-T therapy for B-cell malignancies. The incidence of secondary T-cell lymphoma after CAR-T therapy has been estimated at approximately 0.1%.[3] In comparison, similar or higher rates have been reported in patients with DLBCL who never received CAR-T therapy, with one study reporting a 5-year cumulative incidence of 0.56%.[13] These findings suggest that secondary T-cell lymphoma is not uniquely associated with CAR-T therapy. However, accurate incidence estimation remains challenging, as the poor prognosis in relapsed or refractory DLBCL can obscure the detection of subsequent malignancies due to early mortality or confounding disease progression. Therefore, when relapse is suspected following CAR-T or other therapies for B-cell malignancies, secondary T-cell lymphoma should be considered in the differential diagnosis. Timely rebiopsy is essential to ensure diagnostic accuracy.

Epidemiologic data indicate that secondary T-cell lymphomas may be associated with prior treatments, such as cytotoxic chemotherapy or autologous stem cell transplantation. Patients receiving IEC therapy are often heavily pretreated, and some may harbor latent malignant T-cell clones. Although the overall incidence remains low, several case reports have documented T-cell lymphomas originating from CAR-transduced T-cells,[4-8] especially in patients with pre-existing mutations such as *TET2*.[4,6,8] In our case CAR expression was not confirmed. Although no *TET2* mutation was detected, copy number analysis revealed allelic imbalance at the *TET2* locus (**Figure 3B**), suggesting a possible copy-neutral loss of heterozygosity. Additionally, a *TP53* p.R213X mutation was detected in the lymphoma sample but was absent in the apheresis specimen, indicating it was acquired during IEC therapy. Therapy-related immune and inflammatory pressure—including lymphodepleting conditioning and IEC therapy-induced stress—may have contributed to clonal evolution and malignant transformation.

A key limitation of this case is the unavailability of the infused CAR-T product for direct molecular analysis. Although clonality and the acquisition of *TP53* mutations were confirmed by molecular studies, the exact timing and mechanisms of malignant transformation remain speculative. Furthermore, although CAR expression was undetectable through FCM and qRT-PCR, we cannot definitively exclude the possibility that the CAR transgene was present in the genome but transcriptionally silent owing to unknown regulatory influences.

Despite these limitations, this case provides clinical evidence that pre-existing T-cell clones with malignant potential can evolve into overt T-cell lymphoma during IEC therapy. As CAR-T and BsAbs therapies become more widespread, longitudinal molecular surveillance—including T-cell clonality assessment and mutation profiling—may be crucial for detecting early clonal evolution.

References

1. Thieblemont C, Phillips T, Ghesquieres H, et al. Epcoritamab, a novel, subcutaneous CD3xCD20 bispecific T-cell-engaging antibody, in relapsed or refractory large B-cell lymphoma: dose expansion in a phase I/II trial. J Clin Oncol. 2023;41(12):2238-2247.
2. Hines MR, Knight TE, McNerney KO, et al. Immune effector cell-associated hemophagocytic lymphohistiocytosis-like syndrome. Transplant Cell Ther. 2023;29(7):438.e1-438.e16.
3. Elsallab M, Ellithi M, Lunning MA, et al. Second primary malignancies after commercial CAR T-cell therapy: analysis of the FDA adverse events reporting system. Blood. 2024;143(20):2099-2105.
4. Braun T, Rade M, Merz M, et al. Multiomic profiling of T cell lymphoma after therapy with anti-BCMA CAR T cells and GPRC5D-directed bispecific antibody. Nat Med. 2025;31(4):1145-1153.
5. Ozdemirli M, Loughney TM, Deniz E, et al. Indolent CD4+ CAR T-cell lymphoma after Cilta-cel CAR T-cell therapy. N Engl J Med. 2024;390(22):2074-2082.
6. Kobbe G, Brüggemann M, Baermann BN, et al. Aggressive lymphoma after CD19 CAR T-cell therapy. N Engl J Med. 2024;391(13):1217-1226.
7. Perica K, Jain N, Scordo M, et al. CD4+ T-cell lymphoma harboring a chimeric antigen receptor integration in *TP53*. N Engl J Med. 2025;392(6):577-583.
8. Harrison SJ, Touzeau C, Kint N, et al. CAR+ T-cell lymphoma after Cilta-cel therapy for relapsed or refractory myeloma. N Engl J Med. 2025;392(7):677-685.
9. Henter JI, Horne A, Aricó M, et al. HLH-2004: Diagnostic and therapeutic guidelines for hemophagocytic lymphohistiocytosis. Pediatr Blood Cancer. 2007;48(2):124-131.
10. Alaggio R, Amador C, Anagnostopoulos I, et al. The 5th edition of the World Health Organization Classification of Haematolymphoid Tumours: Lymphoid Neoplasms. Leukemia. 2022;36(7):1720-1748.
11. Ahn JS, Rew SY, Shin MG, et al. Clinical significance of clonality and Epstein-Barr virus infection in adult patients with hemophagocytic lymphohistiocytosis. Am J Hematol. 2010;85(9):719-722.
12. Hamilton MP, Sugio T, Noordenbos T, et al. Risk of second tumors and T-cell lymphoma after CAR T-cell therapy. N Engl J Med. 2024;390(22):2047-2060.
13. Brieghel C, Petersen SL, Brown PN, Niemann CU. Frequency of secondary T-cell lymphoma in chimeric antigen receptor T-cell naïve B-cell lymphoid-lineage cancers is higher than that reported on chimeric antigen receptor T-cell therapy. Haematologica. 2025;110(3):768-771.

Figure Legends

Figure 1 Overview of disease relapses and treatment course leading to epcoritamab therapy.

A Japanese male patient was diagnosed with diffuse large B-cell lymphoma (DLBCL) in 2009 and achieved complete remission following eight cycles of R-CHOP (rituximab, cyclophosphamide, doxorubicin, vincristine, and prednisolone). A first relapse occurred in 2010, and a second complete remission was achieved with R-ICE (rituximab, ifosfamide, carboplatin, and etoposide), followed by autologous stem cell transplantation (ASCT) after R-MCEC (rituximab, ranimustine, carboplatin, etoposide, and cyclophosphamide) conditioning. The patient experienced a second relapse in 2022, prompting lymphocyte apheresis for tisagenlecleucel. This was followed by two cycles of R-GCD (rituximab, gemcitabine, carboplatin, and dexamethasone) and radiation therapy to the cervical lymph nodes in 2023. In April 2023, the patient received tisagenlecleucel following lymphodepleting conditioning with fludarabine and cyclophosphamide (Flu/Cy). A third relapse was confirmed 8 months later by upper gastrointestinal endoscopy, which revealed a duodenal lesion, and by colonoscopy, which showed lesions from the ascending colon to the ileum, both corresponding to areas of fluorodeoxyglucose uptake on positron emission tomography/computed tomography. Treatment with sobuzoxane and rituximab was ineffective, and epcoritamab therapy was initiated in 2024. During epcoritamab treatment, the patient developed pancytopenia and elevated lactate dehydrogenase (LDH) levels. Bone marrow analysis showed an abnormal T-cell population and features consistent with hemophagocytic lymphohistiocytosis (HLH). Despite administration of high-dose corticosteroids and etoposide, HLH proved refractory, and the patient died of multiorgan failure on day 80 of epcoritamab therapy.
Clinical specimens, including residual material from the lymphocyte apheresis procedure and peripheral blood and bone marrow samples with secondary T-cell lymphoma involvement, were stored and later analyzed. FCM: flow cytometry; NGS: next-generation sequencing; PCR: polymerase chain reaction; qRT-PCR; quantitative reverse transcription PCR; *TRG*: *T-cell receptor gamma*.

Figure 2 Bone marrow infiltration of abnormal T-cells demonstrated by Giemsa-stained smear, flow cytometry, and histopathological stainig.

(A) Giemsa staining of the bone marrow showed abnormal lymphocytes (blue arrow) and hemophagocytosis (red arrows). **(B)** Flow cytometry of the bone marrow showed that lymphoid cell population accounted for approximately 20% of the nucleated cells and exhibited CD3-positive (mostly), CD8-positive (mostly), CD5-negative (partly), and CD7-dim phenotype, suggesting the aberrant T-cell proliferation. **(C)** Hematoxylin and eosin staining of the bone marrow clot section showed infiltration of atypical lymphoid cells with irregular nuclear contours (yellow arrows). Immunohistochemical analysis demonstrated that CD3-positive cells exhibited irregular nuclear contours. CD8-positive cells were distributed in a pattern almost identical to that of the irregular CD3-positive infiltrating cells.

Figure 3 Molecular and cytogenetic analyses for the T-cell lymphoma

(A) Flow cytometry (FCM) of peripheral blood mononuclear cells collected during epcoritamab therapy showed no detectable surface expression of the CD19-directed chimeric antigen receptor (CD19-CAR). **(B)** We performed targeted next-generation sequencing on a bone marrow sample with secondary T-cell lymphoma. The genomic coordinates were based on the GRCh37 (hg19) human genome assembly (National Center for Biotechnology Information, NCBI). Our analysis revealed a *TP53* p.R213X mutation (c.637C>T; G-to-A substitution at chr17:7,578,212), two structural deletions in the *T-cell receptor gamma* (*TRG*) region of chromosome 7, and multiple copy number variations including *TET2* and *TP53*. Only representative copy number variation abnormalities are displayed. VAF: variant allele frequency; TCN: total copy number; BAF: B allele frequency. **(C)** Qualitative polymerase chain reaction (PCR) analysis was conducted with primers targeting the *TRG* deletion. Primers were designed to detect a genomic deletion encompassing the region from chr7:38,295,995 to chr7:38,402,471. (i): Three samples were analyzed: sample A, peripheral blood from a healthy volunteer; sample B, an apheresis sample obtained prior to CAR-T therapy; and sample C, a bone marrow specimen from secondary T-cell lymphoma. M: DNA size marker (ladder). PCR amplification produced specific bands in samples B and C. (ii): We used FCM gating to sort CD3-positive and CD3-negative mononuclear cells from the lymphocyte apheresis sample collected prior to CAR-T therapy. The cells were first gated on FSC-A vs SSC-A to exclude debris, and then on FSC-A vs FSC-W to remove doublets. We used PI staining to exclude dead cells. The CD3-positive and CD3-negative populations were then gated for sorting. (iii): Three samples were analyzed: sample D, CD3-negative mononuclear cells obtained prior to CAR-T therapy; sample E, CD3-positive mononuclear cells obtained prior to CAR-T therapy; and sample F, a bone marrow specimen from secondary T-cell lymphoma (same as sample C). M: DNA size marker (ladder). PCR amplification produced specific bands in samples E and F. **(D)** The PCR products from the samples B and C were excised from the gel and subjected to Sanger sequencing to confirm the *TRG* deletion. Sequence alignment comparing reference and sample-derived sequences spanning the *TRG* deletion. The upper sequence represents the reference sequence from NCBI, whereas the lower sequence corresponds to the sample-derived sequence. Red-colored bases denote mismatches or alignment gaps. Both the pre-CAR-T apheresis sample and the secondary T-cell lymphoma sample lacked the genomic region corresponding to chr7:38,295,995–38,402,471. A representative portion of the sequence is shown, highlighting the region flanking the *TRG* deletion. **(E)** Sanger sequencing was performed to confirm the *TP53* mutation in the pre-CAR-T apheresis sample and the bone marrow sample from the secondary T-cell lymphoma**.** A *TP53* c.637C>T mutation at chr17:7,578,212 was detected in the T-cell lymphoma sample but absent in the pre-CAR-T apheresis sample (red arrow).

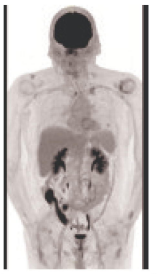

Lymphocyte apheresis:
Stored sample later analyzed for *TRG* by PCR and Sanger sequencing, and for *TP53* by Sanger sequencing, confirming a *TRG* structural deletion and absence of the *TP53* c.637C>T mutation.

Diagnosis of DLBCL — 2009 — R-CHOP

1st relapse of DLBCL — 2010 — R-ICE, ASCT (conditioning: R-MCEC)

2nd relapse of DLBCL — 2022 — Lymphocyte apheresis, R-GCD, Radiation Therapy, Tisagenlecleucel (conditioning: Flu/Cy) — 2023

3rd relapse of DLBCL — Rituximab, Sobuzoxane

Diagnosis of T-cell lymphoma and HLH — 2024 — Epcoritamab

Clinical Course After Epcoritamab Therapy

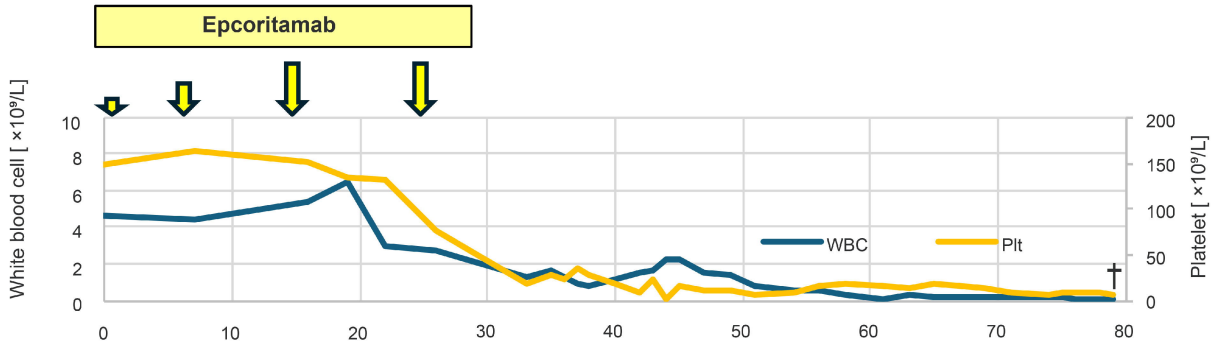

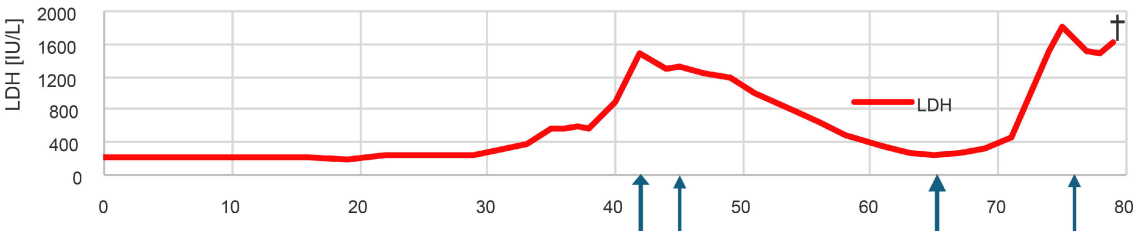

Day 41
Bone marrow:
Abnormal T-cell infiltration and hemophagocytic lymphohistiocytosis.

Day 43
Peripheral blood:
CAR surface expression (FCM) and transgene (PCR) undetectable.

Day 65
Bone marrow:
Stored sample later analyzed by PCR and Sanger sequencing, confirming a structural deletion in the *TRG* locus.

Day 76
Bone marrow:
NGS detected structural deletions in the *TRG* locus and a *TP53* c.637C>T mutation.

A

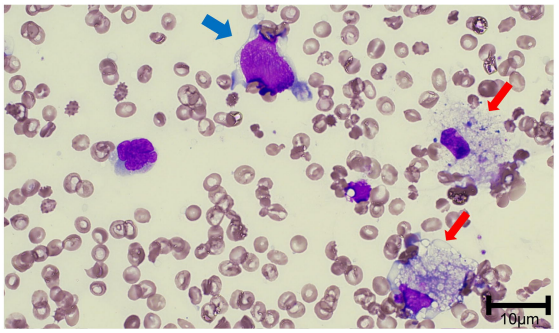

B

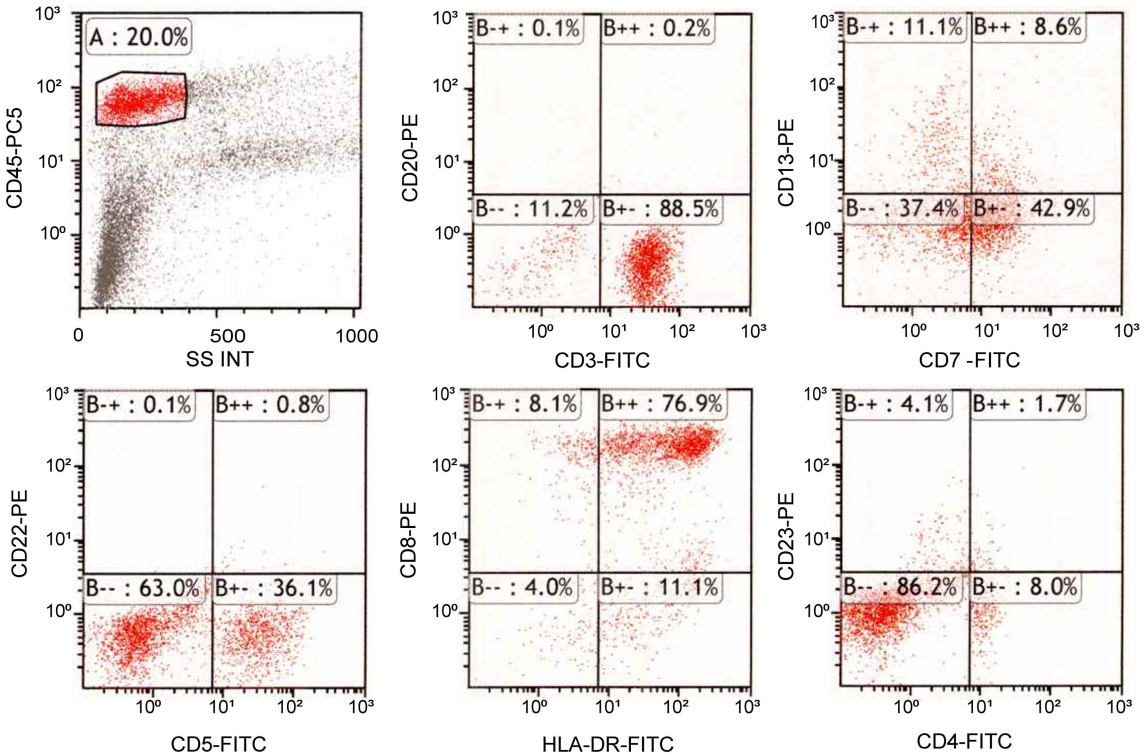

C

Hematoxylin and eosin (×40)

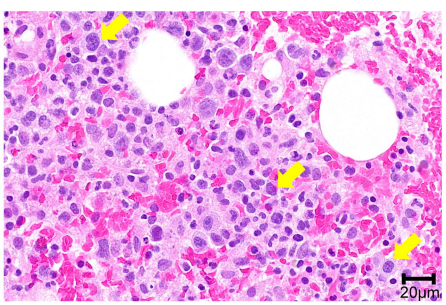

Immunohistochemistry for CD3 (×20)

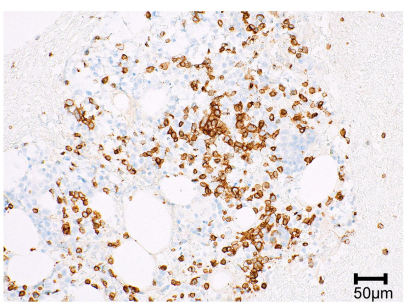

Immunohistochemistry for CD8 (×20)

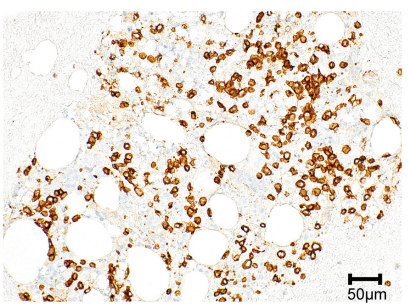

A

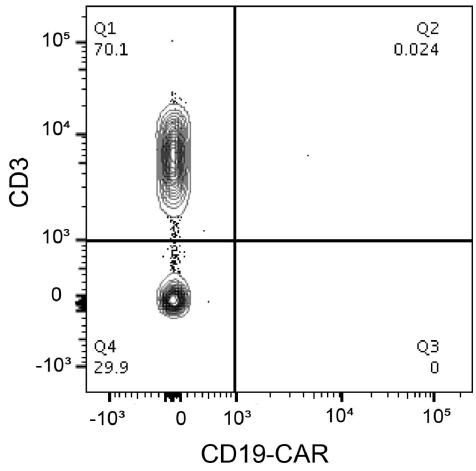

B

Single nucleotide variant calls					
Chromosome	Position	Reference	Alternative	Gene/ Change	VAF
17	7,578,212	G	A	TP53/ p. R213X	0.633
Structural variant calls					
Chromosome 1	Position 1	Chromosome 2	Position 2	Type	VAF
7	38,295,995	7	38,402,471	deletion	0.3278
7	38,315,919	7	38,339,413	deletion	0.5578
Copy number variation calls					
Chromosome	Start	End	TCN	BAF	Gene
4	55,958,742	187,627,698	1.901	0.821	*TET2, NFKB1,* etc.
17	2,916,026	10,740,517	1.912	0.334	*TP53, EIF4A1,* etc.

C

(i) PCR for *TRG* deletion

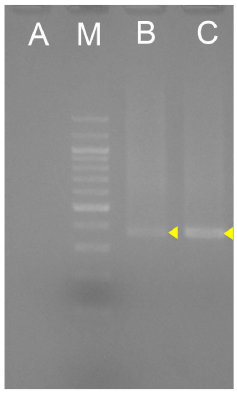

A: peripheral blood from a healthy volunteer

B: apheresis sample of pre-CAR-T therapy

C: secondary T-cell lymphoma

M: DNA size marker (ladder)

(ii)

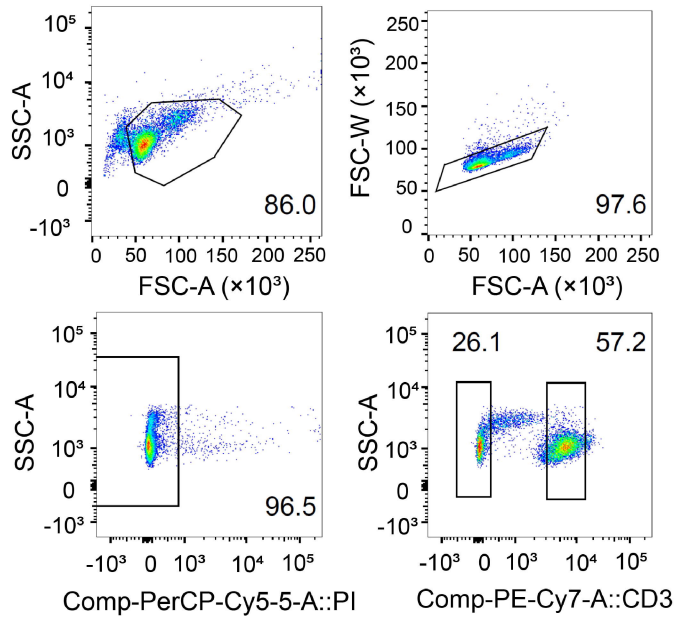

(iii) PCR for *TRG* deletion

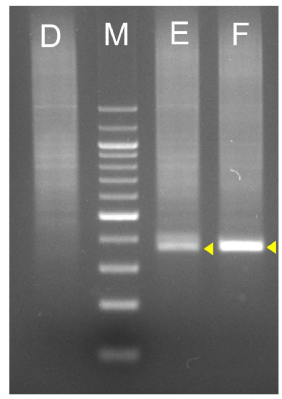

D: CD3-negative mononuclear cells from pre-CAR-T apheresis sample

E: CD3-positive mononuclear cells from pre-CAR-T apheresis sample

F: secondary T-cell lymphoma (same as sample C)

M: DNA size marker (ladder)

D

Apheresis sample of pre-CAR-T therapy

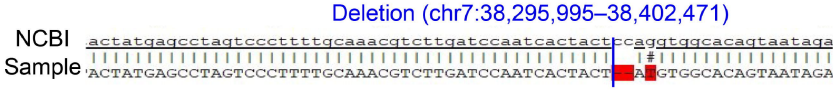

Secondary T-cell lymphoma

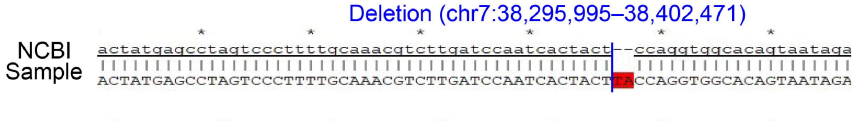

E